Journal of Fluid Science and Technology

Vol. 3, No. 2, 2008

Acoustic Control of an Impinging Planar Jet upon a Wedge*

Shouichiro IIO**, Kohei HIBINO**, Masaharu MATSUBARA*** and Toshihiko IKEDA**

**Department of Environmental Science and Technology, Shinshu University,

***Department of Mechanical Systems Engineering, Shinshu University,

4-17-1 Wakasato, Nagano 380-8553, Japan

E-mail: shouiio@shinshu-u.ac.jp

Abstract

Active control of an impinging jet upon a wedge has been attempted using a sinusoidal excitation of blowing and sucking at the jet exit. The excitation sufficiently enables 'phase-lock', which is synchronization between self-oscillating flow and the excitation, so that hot-wire measurements directly provide phase averaged flow fields and they illustrate appearance of the jet swing in front of the wedge and collision of the jet on one of side of the wedge. It was demonstrated that this control set up is practical not only for illustration of the phase averaged flow field but also for reduction of the edge tone due to the flow oscillation with inverse phase excitation in half of the jet.

Key words: Impinging Jet, Acoustic Control, Hot Wire Measurement, Phase Lock

1. Introduction

Impinging a planar jet upon a wedge gives rise to coherent, self-sustained oscillations, which is called edge tone. The mechanism of edge tone generation has been studied by many researchers in literature, which are summarized in some review papers by Rockwell and Naudasher [1], Rockwell [2], and others. It is known that the generation of the edge tone is due to the self-sustained feedback mechanism created by the interaction of the jet with the wedge. This interaction process is followed by the feedback of the fluctuating pressure to the upstream causing the amplified shear layer instability at the most receptive region near the nozzle exit, which results in vorticity amplification of the jet flow. Measurement of the magnitude of the force on the wedge and the associated sound field were first addressed by Powell [3]. Details of the unsteady nature of the flow on the jet-wedge system are described by Kaykayoglu and Rockwell [4, 5], Sakai et al. [6] and the PIV measurements of the flow field around the wedge are reported by Lin and Rockwell [7].

The purpose of the present study is to examine the effect on the flow structure and the sound pressure level of the local excitation patterns when the phase differences. We clarified the oscillating phenomena of the acoustic controlled jet when the sound pressure level decreases.

2. Experimental apparatus and procedure

A schematic illustration of the experimental set-up is shown in Fig.1. The test section including a wind tunnel and a nozzle are set in the sound proof chamber to attenuate perturbations such as noises from the outside. The dimensions of the chamber are 2.0 m in height, 1.8 m in width and 2.7 m in length. The inner wall of the chamber is covered with glass wool mate of 50 mm thickness except for the floor. The ceiling of the chamber has

*Received 5 Dec., 2007 (No. 07-0806)
[DOI: 10.1299/jfst.3.274]

socket to mount of a wind tunnel consist of a silent duct, flow-rectifying device such as a honeycomb and wire screens. A contraction nozzle is mounted of the wind tunnel exit. The side wall has exhaust opening to connect through a silent duct to the blower setting outside. The blower generates negative pressure by sucking up air in the chamber, then the jet issues from the nozzle exit. The jet velocity is regulated with variable speed motor attached to the blower. In this experiment, the background noise is 57.9 dB for the blower stopping. In the case of free jet without the wedge, the sound pressure level is 75.8 dB. The detailed around the test section is shown in Fig.2. The coordinate system is fixed at the nozzle center, the origin is located at the center of the jet exit, the x-axis is along the flow direction, the y-axis is in the horizontal direction perpendicular to the flow, and the z-axis is in the spanwise direction of the nozzle. The tunnel has a rectangular cross section nozzle. The dimensions of the nozzle are 10 mm in width, w, 150 mm in length, h, the aspect ratio (h/w) of 15, and the contraction ratio is 10.0. The flow velocity at the nozzle exit center, U_0, is 30 m/s (constant) which corresponds to a Reynolds number ($Re = U_0 w/\nu$) of 2.0×10^4, where ν is a kinematic viscosity of air. Sakai et al. [6] suggested that the phase control of an impinging jet on a wedge was enabled by sound irradiation around the jet. In their report, the jet oscillation phenomenon and the growth of dominant frequency component attributed to the edge tone were clearly observed. From these reason, we selected the same experimental conditions, nozzle shape and Reynolds number, to evaluate the effect of local acoustic control on the edge tone.

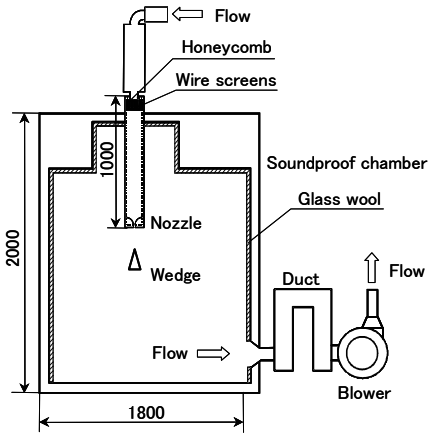

Fig.1 Experimental apparatus

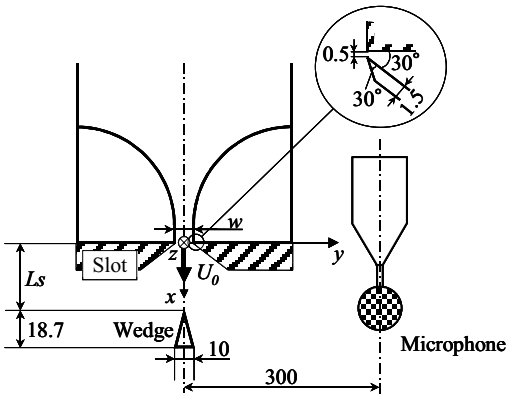

Fig.2 Test section

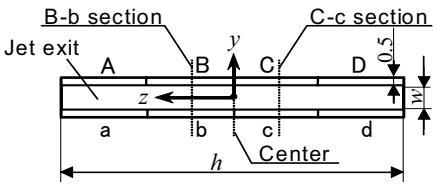

Fig.3 Slot divice

Table 1 Phase patterns

	A	B	C	D	a	b	c	d
1	+	+	+	+	−	−	−	−
2	+	+	−	−	−	−	+	+
3	+	−	+	−	−	+	−	+
4	+	−	−	+	−	+	+	−
5	+	+	+	+	+	+	+	+
6	+	+	−	−	+	+	−	−
7	+	−	+	−	+	−	+	−
8	+	−	−	+	+	−	−	+

The flow velocity at the nozzle exit, U_0, is calculated from the measured pressure drop across the nozzle. The temperature of the flow is kept constant by the air conditioner and the ceiling fan. The impinging wedge is made entirely of Plexiglas. It has an apex angle of 30°, the length of 18.7 mm, the end-width of 10.0 mm and a span of 400 mm thereby extending across the entire test-section. The wedge is situated downstream of the contraction nozzle and is symmetrical with respect to the jet axis. The distance between the wedge apex and the nozzle exit, L_s, can be varied by traversing the wedge. The distance is changed in the range $15 \le L_s / w \le 200$. The slots and two loudspeakers are connected by vinyl pipes having an inner diameter of 9.5 mm, respectively. The power of the loudspeakers used for control is 300 watts and the diameter is 300 mm. The sound pressure level at the location (x, y, z) = (40, 300, 0) is measured by a microphone. A microphone is set as much as possible near the wedge, and this location can ignore influence of a jet flow. The details of the slot structure are shown in a blow up in Fig.2. The slots are made of acrylic, the length is 150 mm. The gap of the slot is 0.5 mm and the slot meets the nozzle exit plane at an angle of 30°. The slot device is shown in Fig.3. The slot is partitioned into eight cells by thin Plexiglas plates shown as Fig.3, it is therefore possible to impose either symmetric or asymmetric excitation on the jet exit. The phase patterns of excitation are shown in Table 1. The sound pressure level is varied with L_S. In case without control, the overall sound pressure level (SPL_N) reached maximum value of 87.0 dB for L_S/w=4, and the dominant frequency of 320 Hz was clearly observed, and hence the excitation frequency for control is set to f_p=320 Hz. The excitation intensity is defined as u_{prms} that the root mean square value of fluctuating velocity at the slot exit. u_{prms}/U_0 is set at 0.5 % . It is note that the streamwise turbulence intensity at the origin was about 0.14 % of U_0=30 m/s. A single hot-wire sensor is utilized for the measurement of the mean and fluctuating velocities. Platinum filament of 2.5 micrometer in diameter and 1 mm in active length is used as hot-wire sensor. The probe is inserted into the flow downstream position by a handmade support without disturbing the flow. The hot-wire probe is operated by constant temperature anemometer. The movement of the sensing probe in the flow field is facilitated by a three-dimensional traversing system that is driven by stepping motors under control of the personal computer. The velocity measurement is conducted three cross sections of the slot device in Fig.3 shown as B-b, C-c and center.

3. Phase average technique

The eduction of the coherent structure as well as interpretation of the data requires introduction of the concept of phase average as suggested by Hussain and Reynolds [8]. In this experiment we used the cyclic position of the speaker signal as a clock for selective sampling, which permitted us to extract the organized wave motion from a background field of finite turbulent fluctuations. We decomposed the fluctuating velocity $u(x, t)$ as the following eqation.

$$u(x,t) = U(x) + \tilde{u}(x,t) + \hat{u}(x,t) \quad (1)$$

Here, U is the streamwise mean velocity, $\tilde{u}$ is the periodic (phase average) velocity and $\hat{u}$ is the turbulence (non-periodic velocity). We also use the definition of the phase average velocity at a particular time θ in the period T of the periodic perturbation.Thus:

$$\tilde{u}(x,\theta) = \lim_{N\to\infty} \frac{1}{N} \sum_{n=1}^{N} \{ u(x,\theta+nT) - U(x) \} \tag{2}$$

The difference between the instantaneous signal and the phase average represents the background random fluctuation, and the difference between the phase average and the time average denotes the (periodic) coherent component. Thus, knowing the period of the induced perturbation, the mean, coherent and random components of the velocity signal can be extracted from the instantaneous total velocity signal.

4. Experimental result

4.1 Sound characteristics

Sound pressure levels with excitation in each phase patterns are shown in Fig.4. *SPL* is overall value of the sound pressure level and SPL_p is the peak sound pressure level at the dominant frequency. The dominant frequency was 320 Hz in all cases. In case of no excitation, the overall sound pressure level SPL_N is 87.0 dB indicated as a solid line, and the peak sound pressure level SPL_{Np} is 83.3 dB shown as a dashed line. Each number of the phase pattern corresponds to each one in table 1. In the case of pattern 1, both *SPL* and SPL_p increase to 95 dB and 93 dB, respectively. This increase is from that the excitation intensifies the flow oscillation. In contrast with pattern 1, excitation with patterns 2, 3, 4 reduces *SPL* and SPL_p suggesting the cancellation between 180 ° phase shifted edge tones generated by the impinging jets to the wedge, whose oscillations are out of phase each other. In cases of patterns 5 to 8, in which the initial disturbance is in-phase, *SPL* and SPL_p do not change drastically. According to an oscilloscope observation the velocity signal at the representative position does not show the phase-lock to the speaker signal. The in-phase initial disturbance is not effective to control of the impinging jet.

The spectra of sound pressure fluctuations with excitation of patterns 1 and 3 and without excitation are shown in Fig.5. In case without excitation, a well-defined peak is evident at f=320 Hz indicating that the natural edge tone consists of a pure sin wave. For pattern 1 excitation, the peak value at the dominant frequency of 320 Hz is ten times larger than SPL_N without excitation. There exist higher harmonics at f = 640 and 960 Hz. For pattern 3 excitation, the peak value of the dominant frequency of 320 Hz decreases to one tenth of the peak value without excitation. Distribution of energy density around the peak is broadband. These spectra also support that the excitation of pattern 1 intensifies the edge

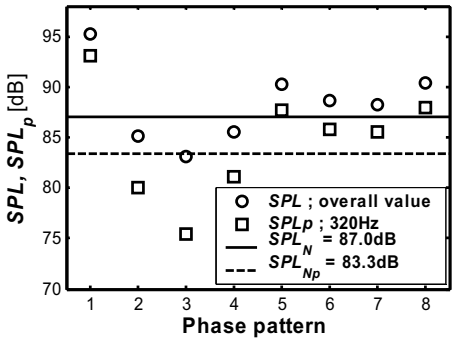

Fig.4 Effect of sound control

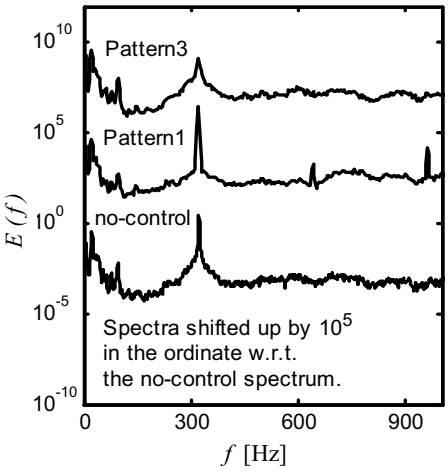

Fig.5 Spectra of the sound pressure fluctuation

tone and that the excitation of pattern 3 reduces the edge tone. In this report, we paid attention to the velocity fields with excitation of pattern 3 when the sound pressure level decreases.

4.2 Velocity measurement

The contour maps of the mean velocity U and root mean square value of the velocity fluctuation u'_{rms} without control are shown in Figs.6(a) and (b). The white areas in the maps are outside of reach of the hot wire measurement due to the slot device. Brighter region indicates higher value. The contour map of U shown in Fig.6(a) almost keeps constant from the jet exit to x/w=3.0. This area is identified a potential core region. The jet width is wider than in the pattern 3 excitation shown in Fig.7(b). The dense contour lines at y/w=0.5 near the jet exit indicates a strong shear layer which extends to the wedge side. The shear layer is somewhat away from the side of the wedge and the shear on the wedge is relatively weak. In the contour map of the velocity fluctuation u'_{rms} shown in Fig.6(b), a large fluctuation of velocity is appeared in $1.5 \le x/w \le 4$ around y/w=0.5, and is spreading in the y direction downstream. The contour maps of the mean velocity U, the periodic velocity fluctuation $\tilde{u}_{rms}$, the non-periodic fluctuation $\hat{u}_{rms}$ with pattern 3 control are shown in Figs.7(a)~(c). The contour maps of U, shown in the top column, shows that mean velocity stays constant in all cross sections from the jet exit to approximately x/w=3.5. The contour line density is higher in Fig.7(b) than other cross-sections. In particular, this tendency is clearly observed on the wedge side, and the jet width is narrower than that of Figs.7(a) and (c). In the contour maps of $\tilde{u}_{rms}$ shown in the middle column, the large value is observed at x/w=4 in Figs.7(a) and (c). In contrast, the large value is not observed at the center (see Fig.7(b)). The tendency of contour maps of $\hat{u}_{rms}$ is almost the same as in Figs.7(a) and (c) shown in the bottom column, these values are relatively small compared with that of Fig.7(b).

In order to understand the instantaneous flow field under the pattern 3 control, the contour maps of the velocity $U+\tilde{u}$ with pattern 3 are shown in Fig.8 as the sequence with the phase progression. These maps are represented using transition from lighter to darker to express values from higher to lower. Tracking the large-scale cluster of high velocity $U+\tilde{u}$ upstream of the wedge, it is recognized that the jet is deflecting in opposite side shown in Figs.8(a) and (c). Correspondingly, the jet of the center section does not deflect with increasing time as shown in Fig.8(b). Therefore the oscillating amplitude is suppressed, and then the sound pressure level decreased.

The streamwise growth of the periodic and non-periodic velocity fluctuations, $\tilde{u}_{rms,max}$ and $\hat{u}_{rms,max}$ as maximum value in all cross-sections (x-y plane), are shown in Fig.9. $\tilde{u}_{rms,max}$ increased exponentially up to x/w=0.8 in all sections where the strong shears existed as shown in Fig.7. It was due to the excitation effect at the nozzle exit. In B-b and C-c sections, $\tilde{u}_{rms,max}$ was slightly decreasing, and increasing in the range x/w=0.8 to 4.0. But $\tilde{u}_{rms,max}$ in Center-section markedly decreased. It was noted that $\tilde{u}_{rms,max}$ in Center-section was one tenth of that in B-b and C-c sections. It could be explained that the opposite-phase oscillation illustrated in Fig.8 suppressed the growth of $\tilde{u}_{rms,max}$ in Center-section. After $\tilde{u}_{rms,max}$ decreasing as far as the wedge apex, the second peak was observed in the range x/w=4.0 to 5.9. It was suggested that some structure impinged periodically on the wedge side. The position of the peaks was x/w=4.2 in B-b and C-c sections, and x/w=5.0 in Center-section. The almost same distribution patterns of $\hat{u}_{rms,max}$ were observed in all cross-sections as shown in Fig.9(b). $\hat{u}_{rms,max}$ increased exponentially up to x/w=1.0 and then showed no change for $1.0<x/w$. There was no clear connection between non-periodic velocity and the jet oscillation. It might be because non-periodic velocity component was generated by the velocity gradient of the shear layer distributed from the nozzle exit to the wedge side.

The contour maps of $U+\tilde{u}$ at y-z plane of x/w=4.25 where the periodic velocity

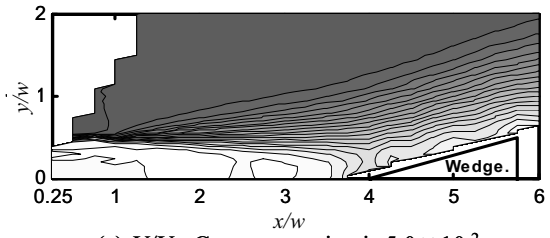

(a) U/U_0. Contour spacing is 5.0×10^{-2}

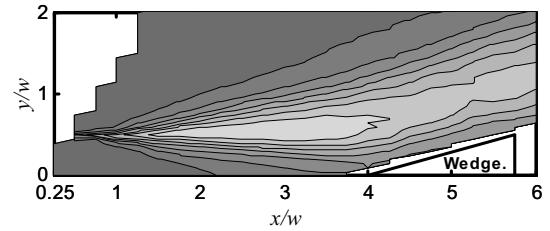

(b) u'_{rms}/U_0. Contour spacing is 2.0×10^{-2}

Fig.6 Contour maps of the decomposed velocity without control

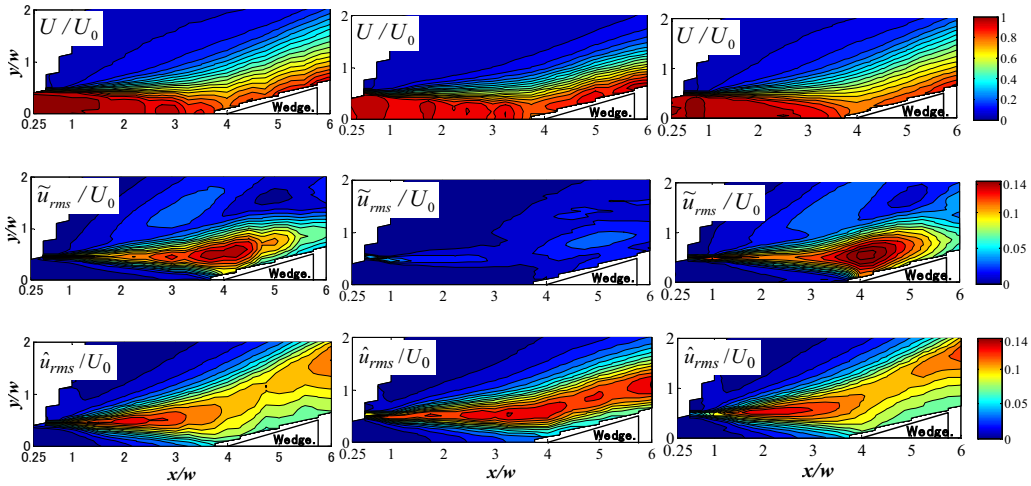

(a) z/w=1.9 (B-b section) (b) z/w=0 (Center) (c) z/w=-1.9 (C-c section)

Fig.7 Contour maps of U/U_0, $\tilde{u}_{rms}/U_0$ and $\hat{u}_{rms}/U_0$ with control of pattern 3

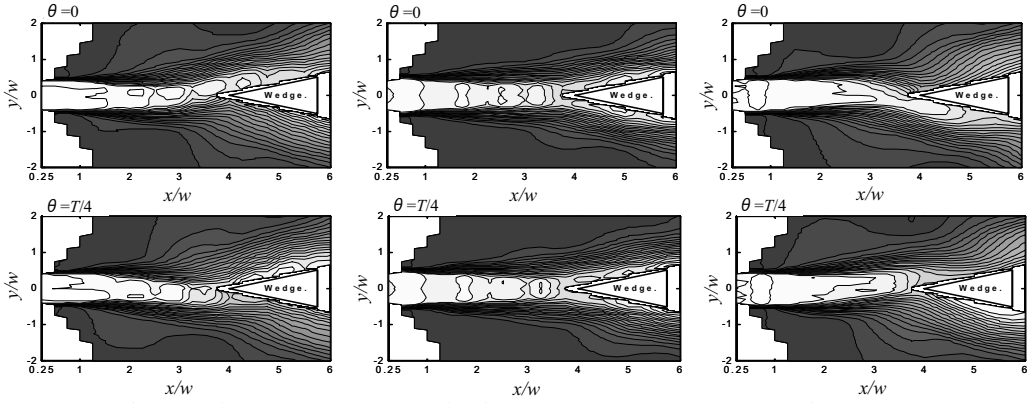

(a) z/w=1.9 (B-b section) (b) z/w=0 (Center) (c) z/w=-1.9 (C-c section)

Fig.8 Contour maps of $(U+\tilde{u}(\theta))/U_0$ with control of pattern 3. Contour spacing are 5.0×10^{-2}

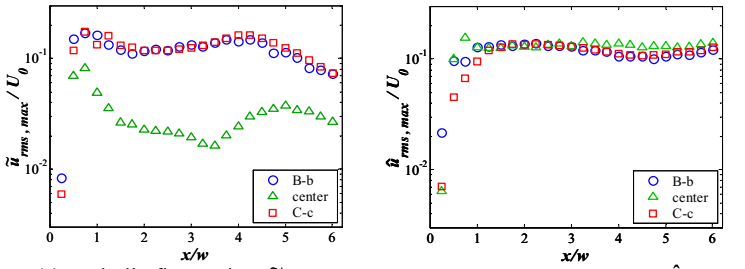

(a) Periodic fluctuation $\tilde{u}_{rms,max}$ (b) Non-periodic fluctuation $\hat{u}_{rms,max}$

Fig.9 Growth of the velocity fluctuations with control of pattern 3

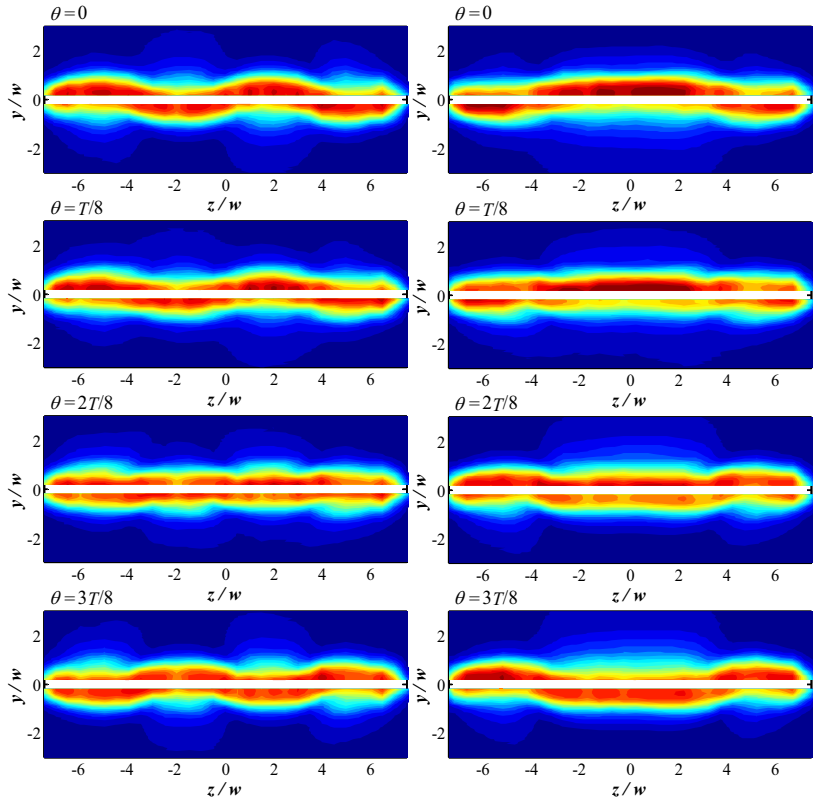

(a) Pattern 3 (b) Pattern 4

Fig.10 Contour maps of $(U+\tilde{u}(\theta))/U_0$ with control. x/w=4.25, Contour spacing are 1.0×10^{-2}

fluctuation reached maximum for pattern 3 were shown in Fig.10 as the sequence with the phase progression. The clear oscillation in the y-direction of the large-scale cluster with high velocity was observed for both excitation patterns 3 and 4. These jet behaviors were synchronized with each excitation pattern as shown in Table 1.

From mentioned above, the decrease of the edge tone was attributed to the anti-phase oscillation along the spanwise direction of the nozzle.

5. Conclusions

The performance and mechanism of an acoustic control applied to flow oscillation in a jet-wedge system were investigated experimentally. The following conclusions can be drawn:

(1) The excitation sufficiently enables 'phase-lock', which is synchronization between self-oscillating flow and the excitation, so that hot-wire measurements directly provide

phase averaged flow fields and they illustrate appearance of the jet swing in front of the wedge and collision of the jet on one of side of the wedge.

(2) The sound pressure level decreased with inverse phase excitation in half of the jet.

(3) When the sound pressure level decreases, opposite phase oscillation was observed in the spanwise direction of the nozzle.

References

(1) Rockwell, D., Naudascher, E., Self-sustained oscillations of impinging free shear layers, *Annual Review of Fluid Mechanics*, Vol.11 (1979), pp.67-94.

(2) Rockwell, D. O., Transverse oscillations of a jet in a jet-splitter system, *Transaction of ASME, Series D* (1972), pp.675-681.

(3) Powell, A., On the edgetone, *Journal of Acoustical Society of America*, Vol.33, No.4 (1961), pp.395-409.

(4) Kaykayoglu, R., Rockwell, D., Unstable jet-edge interaction: part 1 Instantaneous pressure fields at a single frequency, *J. Fluid Mech.*, Vol.169 (1986), pp.125-149.

(5) Kaykayoglu, R., Rockwell, D., Unstable jet-edge interaction: part 2 multiple frequency pressure fields, *J. Fluid Mech.*, Vol.169 (1986), pp.151-172.

(6) Sakai G., Matsubara M., Ikeda T., Tsuchiya Y., Phase-control of an impinging jet by a sound wave, *Transactions of the Japan Society of Mechanical Engineers, Series B*, Vol.70, No.697 (2004), pp.2355-2362.

(7) J. -C. Lin and D. Rockwell, Oscillations of a turbulent jet incident upon an edge, *Journal of Fluids and Structures*, Vol.15 (2001), pp.791-829.

(8) Hussain, A. K. M. F., Reynolds, W. C., The mechanics of an organized wave in turbulent shear flow, *J. Fluid Mech.*, Vol.41, No.2 (1970), pp.241-258.